1985

Interril Soil Erosion, Part II. Testing and Use of Model Equations

John E. Gilley
University of Nebraska-Lincoln, john.gilley@ars.usda.gov

D. A. Woolhiser
United States Department of Agriculture

D. B. McWhorter
Colorado State University, dave@engr.colostate.edu

Interrill Soil Erosion - Part II: Testing and Use of Model Equations

J. E. Gilley, D. A. Woolhiser, D. B. McWhorter

| MEMBER | MEMBER | ASSOC. MEMBER |
| ASAE | ASAE | ASAE |

ABSTRACT

LABORATORY measurements were made of interrill erosion as affected by varying overland flow discharge and slope steepness. Soil detachment and sediment transport capacity relations were then evaluated using experimentally obtained information.

The model equations were utilized to further characterize interrill soil erosion. The overland flow region over which the model equations are applicable for a disturbed Nunn clay loam soil was determined from laboratory tests and critical shear stress analyses. The influence of slope length on interrill erosion was also examined.

INTRODUCTION

Equations describing overland flow depth, rainfall induced soil detachment and sediment transport capacity on interrill areas have been previously identified (Gilley et al., 1985). Non-dimensional forms of each of the model equations were evaluated separately. Research data to allow testing of the interactive effects of the equations were not available. Therefore, a laboratory study was initiated to generate information allowing more comprehensive evaluation of the model equations. The objectives of this investigation were to (a) measure the effects of varying discharge and slope steepness on interrill soil erosion, (b) test the previously identified model equations on the experimentally obtained information, (c) identify the interrill overland flow range and (d) examine the influence of slope length on interrill erosion.

METHODS AND MATERIALS USED IN THE EXPERIMENTAL STUDY

The experimental study was performed using a soil pan positioned under a rainfall simulator. In portions of the study, inflow was introduced at the top of the test section to simulate longer slopes. Samples were collected at five minute intervals during the runoff events to determine water and soil loss. The soil water mixture was dried in an oven and water loss was calculated as the

difference between total measured runoff and soil loss.

Nunn clay loam soil was selected for the experimental study. The Nunn clay loam series usually consists of deep soils with large water holding capacities. The soil which was removed from the top few inches of a farmed site was sieved through a 14 mm mesh screen at time of collection and air dried prior to testing. The particle size for which 50% of the dispersed Nunn clay soil was finer was found to be approximately 16 μm.

The design, construction and calibration of the rainfall simulator used in this study is described by Peterson (1977). The simulator consists of capillary tubing drop formers inserted into rectangular plastic reservoirs. The framework used to support the plastic reservoirs allows the 3.6 mm diameter drops to approach approximately 77% of their terminal velocity. A rainfall intensity of approximately 64 mm/h was used for each of the rainfall simulation runs. A random distribution of raindrops was achieved by oscillating the rainfall modules and by using two opposing electric fans to generate turbulent air movement between the drop formers and the soil pan.

The soil pan design and soil preparation techniques described by Lattanzi et al. (1974) were used in the present study. The soil pan consisted of a 61 by 61 cm test area surrounded by a border region to compensate for splash erosion. The central test section was separated from the border area by vertical sheet metal strips. Soil was placed in the pans in three successive 2.5 cm layers. Each layer was compressed by hand using a wooden block. A fourth layer was applied on the top and leveled without compressing resulting in a total soil sample depth of approximately 7.6 cm. The soil in each of the compartments was replaced after each series of initial, wet and inflow test runs.

The first rainfall application (initial run) was applied at existing soil water conditions with a second simulation run (wet run) conducted approximately 24 h later. Both the initial and wet runs lasted for 60 min. Additional testing (inflow test runs) was conducted approximately 24 h after completion of the wet run. A summary of the rainfall simulation test runs is shown in Table 1.

The inflow rates within a test series were selected prior to testing with each inflow rate maintained for 20 min. Differences between subsequent inflow rates within a series were similar. Inflow rates were varied between test series depending upon slope gradient and the quantity of discharge required to initiate soil rilling in previous tests. Clear inflow was used in all cases. Rill establishment was determined by visual observation of surface soil conditions. In general, rill formation proceeded quite rapidly after introduction of a critical discharge rate. Inflow tests runs were made over equivalent slope lengths ranging from approximately 0.6 to 9.1 m. Additional

TABLE 1. RAINFALL SIMULATION TEST RUNS*

Slope, %	Replication	Initial run	Wet run	Average runoff rate, mm/h				
				Inflow level				
				Zero	Level 1	Level 2	Level 3	Level 4
1	1	41.8	—	57.9	266.4	428.8	548.2	762.0
	2	43.4	59.4	—	242.7	405.2	501.5	738.4
6	1	38.2	58.4	56.1	254.0	422.9	584.8	655.7
	2	37.0	58.0	53.8	218.0	344.4	435.3	523.4
	3	—	—	47.3	196.7	345.0	425.9	529.9
12	1	47.8	54.9	53.8	207.3	431.2	661.6	—
	2	50.2	56.5	54.3	121.1	222.1	285.3	—
20	1	52.9	53.5	48.4	169.5	301.3	441.8	516.3
	2	41.2	51.7	46.1	155.4	258.7	331.4	401.7
	3	—	—	42.5	92.1	142.4	195.5	—

*Rainfall intensity approximately 63.5 mm/h.

details concerning the experimental study are given by Gilley (1982).

RESULTS OF THE EXPERIMENTAL STUDY

Average runoff rates during the initial and wet simulation runs are presented in Table 1. Runoff during the initial run usually began after a period of at least 15 min and then slowly increased throughout the rainfall event. In contrast, runoff began rapidly for the wet run, reaching a nearly steady state condition soon after initiation of rainfall.

Soil loss rates for the initial and wet simulation runs are compared in Figs. 1 and 2 with information obtained by Lattanzi et al. (1974) for Russel silt loam, and Harmon and Meyer (1978) for Providence silt loam soil. For each of the three soils, soil loss increased with slope steepness. Soil loss rates obtained in the present investigation were generally smaller than the values reported by Lattanzi et al. (1974) and greater than the rates reported by Harmon and Meyer (1978).

The effects of varying discharge and slope steepness on interrill soil erosion for the Nunn clay loam soil investigated in this study are shown in Figs. 3 to 6. In most cases, the soil loss and runoff rates are the average

of four samples. Greater discharge rates resulted in increased soil loss in some instances and decreased soil loss in others.

Monke et al. (1977) found consistently greater interrill erosion from increased overland flow. However, most of the discharge rates used by Monke et al. (1977) were much smaller than those employed in this study. It is possible that sediment transport capacity was the limiting soil loss variable for smaller runoff quantities. As discharge rate increases, water depth would also be expected to become greater causing less raindrop induced soil detachment. As a consequence, soil detachment could have become the soil loss constraint for the larger runoff quantities used in this study.

The discharge rate required for initiation of rilling was found to be somewhat variable for a particular slope. In general, rilling began at smaller discharge rates as the slope increased. A discharge quantity near the capacity of the inflow system was not large enough to initiate rilling on the 1% slope.

TESTING OF THE MODEL EQUATION

Laboratory data from the inflow test runs were used to evaluate the previously defined model equations. Since
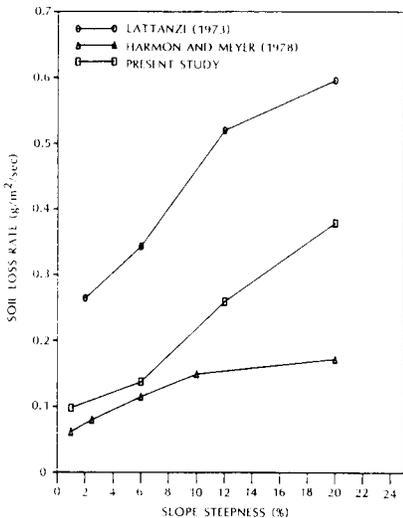

Fig. 1—Effect of slope steepness on soil lost in runoff for the initial run.
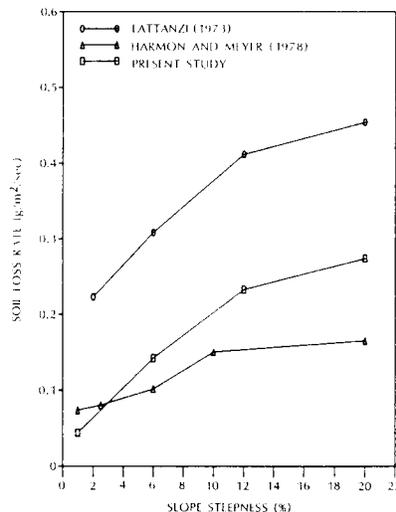
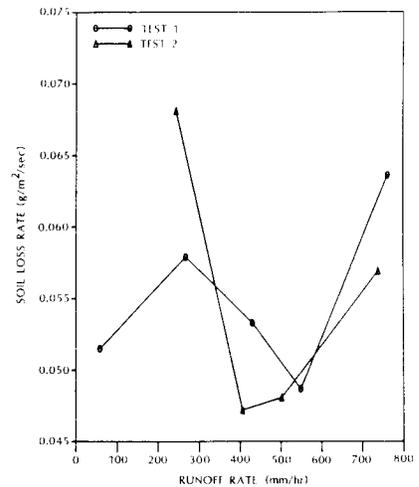Fig. 2—Effect of slope steepness on soil lost in runoff for the wet run.

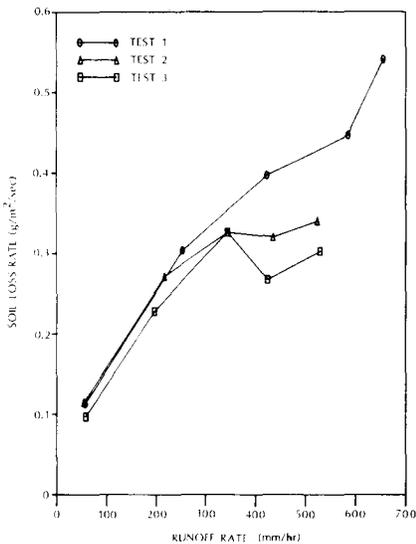Fig. 3—Soil loss rate vs. runoff rate - 1% slope.

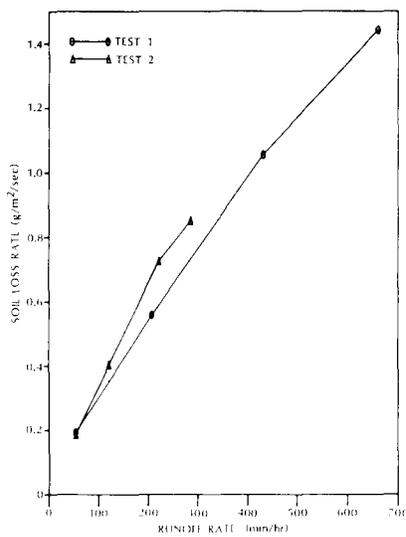Fig. 4—Soil loss rate vs. runoff rate - 6% slope.

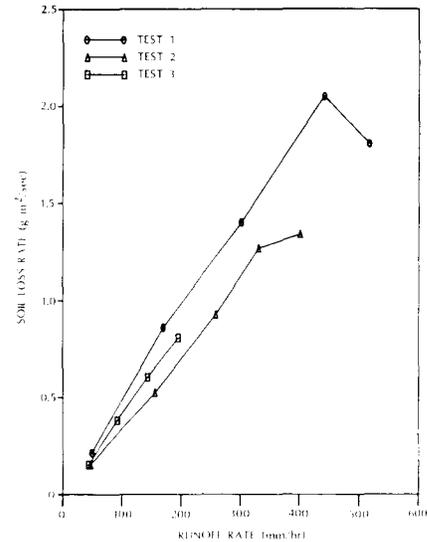Fig. 5—Soil loss rate vs. runoff rate - 12% slope.

Fig. 6—Soil loss rate vs. runoff rate - 20% slope.

the model equations were derived for interrill flow conditions, only those tests which occurred prior to initiation of rilling were used in testing of the equations.

The Darcy-Weisbach friction factor, f, for each inflow test series was determined using the following equation:

$$f = \frac{b\ i^c + k_w}{R_n} \quad \dotfill [1]$$

where b and c are regression constants (Shen and Li, 1973); i = rainfall intensity; k_w = surface roughness coefficient; and R_n = Reynolds number. Reynolds number is given as:

$$R_n = \frac{q}{\nu} \quad \dotfill [2]$$

where q = flow rate of combined flow per unit width and ν = kinematic viscosity of water. For rainfall intensities reported in mm/h, values of b and c in equation [1] are given as 7.21 and 0.41, respectively (Shen and Li, 1973). The surface roughness coefficient for the bare soil surface was assumed to equal 200 (Gilley et al., 1985) Kinematic viscosity of water was determined from measured values of water temperature. Rainfall intensity and flow rate were measured experimentally.

Once the Darcy-Weisbach friction factor and flow rate were determined, the value of water depth, y was calculated for a particular slope gradient, S, using the following relation:

$$y = \left[\frac{f\ q^2}{8\ g\ S}\right]^{1/3} \quad \dotfill [3]$$

where g = gravitational acceleration. Runoff velocity, V_f, was then obtained from the continuity equation:

$$q = V_f\ y \quad \dotfill [4]$$

The hydraulic variables y and V_f were required to test the soil detachment and sediment transport capacity relations.

Raindrop detachment from several drops, D_s, is given as (Gilley et al., 1985):

$$D_s = 0.2\ K_d\ \rho\ \cos^2\ \theta \sum_{i=1}^{n} a_i\ V_i^2 \left(\frac{d_i}{y}\right)^{1.83} \quad \dotfill [5]$$

where K_d = soil detachment factor; ρ = density of water; θ = slope angle; a_i = number of drops in the ith class; d_i = mean drop diameter in that class; and V_i = velocity of drops with diameter, d_i. Sediment transport capacity of flow is represented by the following equation:

$$T = K_t\ (\gamma\ y\ S)\ V_f \quad \dotfill [6]$$

where K_t = sediment transport factor and γ = specific weight of water.

Equation [5] and [6] were first used to determine K_d and K_t, respectively, for the soil used in the experimental study. The soil detachment and sediment transport factors were calculated from a portion of the experimental data. The model equations were then used to compare predicted and measured soil loss rates for the remainder of the experimental data.

In evaluating the soil detachment and transport capacity equations, it was assumed that the ability of the flow to transport detached soil particles was the constraint at zero and level 1 inflow rates for each of the slope gradients. The suitability of this assumption was evaluated by comparing predicted and measured soil loss rates. At greater inflow rates the transport capacity of the flow increased rapidly while detachment decreased causing soil detachment to become the limiting parameter.

Predicted versus measured soil loss rates are shown in Fig. 7. Linear regression analyses of the data shown in Fig. 7 are given in Table 2. Students-t test was used to evaluate the hypotheses that the regression coefficient equals one and the intercept equals zero at the 99% confidence level. The regression was highly significant with the regression coefficient found to be not significantly different from one nor the intercept significantly different from zero. Thus, analyses of experimental information collected in this study suggest
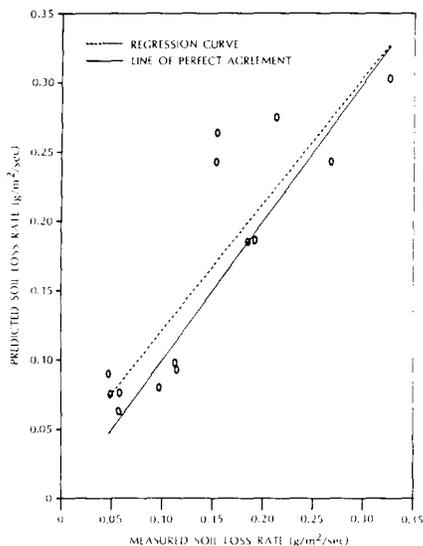
156

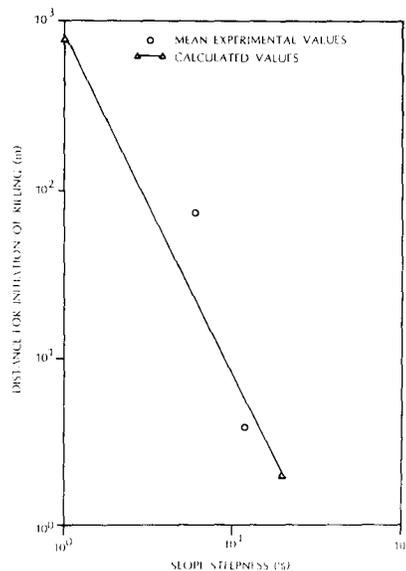Fig. 7—Predicted vs. measured soil loss rates.

Fig. 8—Distance for initiation of rilling vs. slope steepness.

that equations [5] and [6] are appropriate relations for describing interrill soil detachment and sediment transport capacity, respectively.

INTERRILL OVERLAND FLOW RANGE

The present study was conducted to evaluate interrill soil erosion. Consequently, the experimental results are applicable to only a limited overland flow region. Analysis of flow shear stress was utilized to estimate this overland flow range.

The critical shear stress, τ_c, required for the beginning of motion of soil material is given by:

$$\tau_c = \gamma \, y \, S \qquad \qquad [7]$$

where γ = specific weight of water and the other quantities are as previously defined. Substituting equations [1], [2] and [3] into equation [7] and solving for q, the following relation is obtained:

$$q = \left[\frac{\tau_c}{\gamma}\right]^3 \frac{8\,g}{S^2 \, (b \, i^c + k_w) \, \nu} \qquad \qquad [8]$$

Equation [8] can be used to determine the flow rate at which critical shear stress occurs. Flow rate at a particular downslope distance can be obtained from the following relation:

$$q = i_e \, x \qquad \qquad [9]$$

where i_e = rainfall excess and x = distance in the main flow direction. Rainfall excess is given by:

$$i_e = i - i_f \qquad \qquad [10]$$

where i_f = infiltration rate. Substituting equations [9] and [10] into equation [8] and solving for x yields the following relation:

$$x = \left[\frac{\tau_c}{\gamma}\right]^3 \frac{8\,g}{S^2 \, (b \, i^c + k_w) \, \nu \, (i - i_f)} \qquad \qquad [11]$$

The downslope distance at which critical shear stress occurs can be determined from equation [11].

During the experimental inflow test runs, each test rate was maintained for 20 minutes. Rilling usually began on the 6, 12 to 20% slopes soon after introduction of a critical discharge quantity. However, for tests 1 and 3 on a 20% slope, rilling began only after 15 min of inflow application at what proved to be the critical rate. These discharge quantities were averaged to obtain the threshold value for initiation of rilling for the particular soil and slope conditions. A critical shear stress of 0.151 kg/m² was calculated from equation [8] for the Nunn clay loam soil used in the present study.

Equation [11] was used to calculate the distance required for initiation of rilling as shown in Fig. 8. Included are average observed experimental values obtained on 6 and 12% slopes. For the ten initial inflow test runs, a mean infiltration rate of 12.5 mm/h was determined. Thus, an average rainfall excess of 51.0 mm/h would be expected for the Nunn clay loam soil at a rainfall intensity of 63.5 mm/h. A value of k_w = 200 and a water temperature of 20°C was assumed in development of Fig. 8.

The overland flow length required for establishment of critical shear stress was found to vary by two orders of magnitude as the slope increased from 1 to 10%. Rilling

TABLE 2. STATISTICAL ANALYSES OF PREDICTED VERSUS MEASURED SOIL LOSS RATES.

Dependent variable	Regression equation	Coefficient of determination, r^2	F	β_1		β_0	
				Students-t	Standard error	Students-t	Standard error
Predicted soil loss rate	Predicted soil loss rate = 0.914 (measured soil loss rate) + 0.030	0.767	39.7	-0.593	0.145	0.034	0.870

would be expected to occur within a few meters of the uphill boundary on the disturbed Nunn clay loam soil for slopes in excess of 15%. In contrast, in the absence of concentrated flow, rilling would probably occur only after several hundred meters on relatively flat surfaces.

It is important to note that the information presented in Fig. 8 is only applicable for the Nunn clay soil used in the experimental study. Critical shear stress would be expected to be influenced by the degree of soil disturbance. The critical shear stress values obtained from data collected under existing laboratory conditions would probably vary from field measurements. Distances required for initiation of rilling as shown in Fig. 8 were calculated assuming broad sheet flow. The existence of concentrated flow, which is found under most field situations, would reduce the downslope distance required for rill formation.

INFLUENCE OF SLOPE LENGTH ON INTERRILL EROSION

Slope length affects interrill soil erosion because water depth, a variable found in both the soil detachment and overland flow transport capacity relationships, increases with distance from the top of the slope. From information on flow rate given in equation [9] and water depth given in equation [3] raindrop detachment and sediment transport capacity at a particular slope length can be calculated from equations [5] and [6], respectively. These same equations can also be used to evaluate the effects of slope steepness on soil erosion at a particular downslope distance.

The effects of varying slope length on soil loss for slopes of 1, 6 and 12% are shown in Figs. 9, 10 and 11, respectively. In solving the above equations, values of the following variables were used: $i = 63.5$ mm/h, $i_c = 51.0$ mm/h, $k_w = 200$ and $v = 1.004 \times 10^{-6}$ m²/s.

For the 1% slope, as shown in Fig. 9, transport capacity was the limiting variable through a slope length of approximately 17 m. For greater distances from the top of the slope, raindrop detachment served as a soil loss constraint.

For a 6% slope overland flow transport capacity was found to be the limiting variable through a slope length

of approximately 11 meters (Fig. 3). Soil detachment then became the soil loss constraint through a distance of 22 m, the approximate slope length for initiation of rilling.

The downslope distance for rill formation on a 12% slope was estimated as approximately six meters. As a result, sediment transport capacity would serve as the limiting variable throughout the interrill range as shown in Fig. 4. Interrill soil loss on a 12% slope would be expected to increase in a linear fashion with downslope distance.

SUMMARY AND CONCLUSIONS

A rainfall simulator was used to measure interrill runoff and erosion under laboratory conditions for a Nunn clay loam soil. Discharge and slope steepness were included as experimental variables. Inflow was added at the top of the test section in a portion of the study to simulate greater slope lengths.

Soil loss consistently increased with slope steepness when inflow was not added. Greater discharge rates, resulting from addition of inflow, caused larger erosion rates in some instances and reduced rates of erosion in others. In general, rilling was observed to occur at smaller discharge rates as slope steepness was increased.

The experimentally obtained information was used to test previously identified model equations. In general, predicted soil loss rates agreed well with measured data. Analyses of experimental information collected in the present study suggest that previously identified detachment and transport relations are appropriate for estimating interrill soil erosion.

The interrill overland flow range for the Nunn clay loam soil used in this study was determined by experimental and analytic evaluation of critical shear stress. The overland flow length required for establishment of critical shear stress is expected to change from a few meters to several hundred meters as slope gradient is decreased from 10 to 1%.

Slope length affects interrill soil erosion because water depth increases with downslope distance. Water depth in turn influences soil detachment and overland flow sediment transport capacity. Soil erosion at a particular
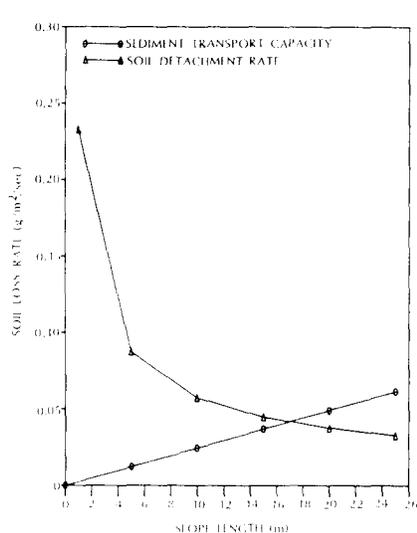

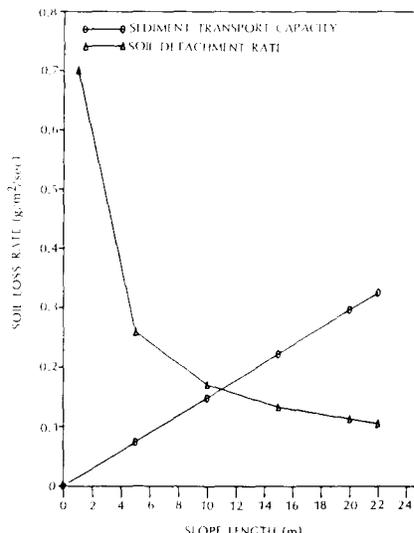
Fig. 9—Soil loss rate vs. slope length - 1% slope.

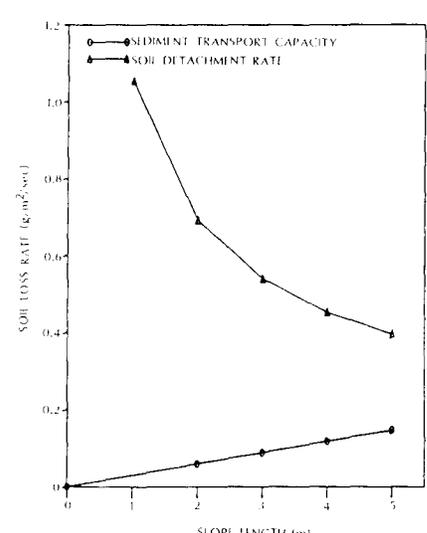Fig. 10—Soil loss rate vs. slope length - 6% slope.

Fig. 11—Soil loss rate vs. slope length - 12% slope.

downslope distance is dictated by soil detachment or sediment transport capacity characteristics existing at that particular location.

References

1. Gilley, J. E. 1982. Soil erosion by sheet flow. Ph.D. Thesis. Colorado State University, Fort Collins, 146 pp.

2. Gilley, J. E, D. A. Woolhiser and D. B. McWhorter. 1985. Interrill soil erosion - Part I. Development of model equations. TRANSACTIONS of the ASAE (this issue).

3. Harmon, W. C. and L. D. Meyer. 1978. Cover, slope and rain intensity affect interrill erosion. Proc. Mississippi Water Resources Conference, Jackson, MS, pp. 9-15.

4. Lattanzi, A. R., L. D. Meyer and M. F. Baumgardner. 1974. Influences of mulch rate and slope steepness on interrill erosion. Soil Science Society of American Proceedings 38(6):946-950.

5. Monke, E. J., H. J. Marelli, L. D. Meyer, J. F. DeJong. 1977. Runoff, erosion and nutrient movement from interrill areas. TRANSACTIONS of the ASAE 20(1):58-61.

6. Peterson, R. J. 1977. Laboratory simulation of soil erosion. M. S. Thesis. Colorado State University, Fort Collins, 70 pp.

7. Shen, H. W. and R. M. Li. 1973. Rainfall effect on sheet flow over smooth surface. J. Hyd. Div. Proc. ASCE 99(HY-5):1367-1386.

LIST OF SYMBOLS

a_i Number of drops of a particular diameter, d_i

b Constant relating rainfall induced roughness to rainfall intensity, $k_r = b\ i^c$

c Constant relating rainfall induced roughness to rainfall intensity, $k_r = b\ i^c$

d_i Drop diameter of a particular size class, (length)

D_s Raindrop detachment from several drops, (mass/area/time)

f Darcy-Weisbach friction coefficient

F F - distribution

g Gravitational acceleration, (length/time^2)

i Rainfall intensity, (length/time)

i_e Rainfall excess (length/time)

i_f Infiltration rate, (length/time)

k_w Surface roughness in friction coefficient equation, $f_w = k_w/R_n$

K_d Soil detachment factor, (time/length)

K_t Sediment transport factor, (time^2/length^2)

q Flow rate per unit width, (volume/time/width)

R_n Reynolds number, $R_n = V_f\ y/\nu$

S Channel bottom slope

T Sediment transport capacity of flow, (mass/width/time)

V_i Impact velocity of drop with diameter, d_i, (length/time)

V_f Flow velocity, (length/time)

x Distance in the main flow direction, (length)

y Flow depth, (length)

β_o Intercept in regression equation

β_1 Regression coefficient in regression equation

γ Specific weight of water, (force/length)

θ Slope angle

ν Kinematic viscosity of water, (length^2/time)

ρ Density of water, (mass/volume)

τ_c Critical shear stress, (force/length^2)